This document is downloaded from DR-NTU (https://dr.ntu.edu.sg)
Nanyang Technological University, Singapore.

Germanium p-i-n avalanche photodetector fabricated by point defect healing process

Baek, Jung Woo; Kim, Gwang Sik; Yu, Hyun-Yong; Park, Jin-Hong; Shim, Jae Woo; Kang, Dong-Ho; Yoo, Gwangwe; Hong, Seong-Taek; Jung, Woo-Shik; Kuh, Bong Jin; Lee, Beomsuk; Shin, Dongjae; Ha, Kyoungho

2014

Shim, J., Kang, D. H., Yoo, G., Hong, S. T., Jung, W. S., Kuh, B. J., et al. (2014). Germanium p-i-n avalanche photodetector fabricated by point defect healing process. Optics Letters, 39(14), 4204-4207.

https://hdl.handle.net/10356/104840

https://doi.org/10.1364/OL.39.004204

© 2014 Optical Society of America. This paper was published in Optics Letters and is made available as an electronic reprint (preprint) with permission of Optical Society of America. The paper can be found at the following official DOI: [http://dx.doi.org/10.1364/OL.39.004204]. One print or electronic copy may be made for personal use only. Systematic or multiple reproduction, distribution to multiple locations via electronic or other means, duplication of any material in this paper for a fee or for commercial purposes, or modification of the content of the paper is prohibited and is subject to penalties under law.

Downloaded on 19 Jun 2024 23:10:41 SGT

Germanium p-i-n avalanche photodetector fabricated by point defect healing process

Jaewoo Shim,[1] Dong-Ho Kang,[1] Gwangwe Yoo,[1] Seong-Taek Hong,[1] Woo-Shik Jung,[2] Bong Jin Kuh,[3] Beomsuk Lee,[3] Dongjae Shin,[3] Kyoungho Ha,[3] Gwang Sik Kim,[4] Hyun-Yong Yu,[4] Jungwoo Baek,[5] and Jin-Hong Park[1,*]

[1]*School of Electronics and Electrical Engineering, Sungkyunkwan University, Suwon 440-746, South Korea*

[2]*Department of Electrical Engineering, Stanford University, Stanford, California 94305, USA*

[3]*Semiconductor R&D Center, Samsung Electronics Co., Ltd., Gyeonggi-Do 445-701, South Korea*

[4]*School of Electrical Engineering, Korea University, Seoul 136-701, South Korea*

[5]*School of Mechanical & Aerospace Engineering, Nanyang Technological University, Singapore 639798, Singapore*

**Corresponding author: jhpark9@skku.edu*

Received April 24, 2014; accepted May 27, 2014; posted June 12, 2014 (Doc. ID 210792); published July 10, 2014

In this Letter, we report Ge p-i-n avalanche photodetectors (APD) with low dark current (sub 1 μA below $V_R = 5$ V), low operating voltage (avalanche breakdown voltage = 8–13 V), and high multiplication gain (440–680) by exploiting a point defect healing method (between 600°C and 650°C) and optimizing the doping concentration of the intrinsic region (p-type $\sim 10^{17}$ cm^{-3}). In addition, Raman spectroscopy and electrochemical capacitance voltage analyses were performed to investigate the junction interfaces in more detail. This successful demonstration of Ge p-i-n APD with low dark current, low operating voltage, and high gain is promising for low-power and high-sensitivity Ge PD applications. © 2014 Optical Society of America

OCIS codes: (040.3060) Infrared; (040.1345) Avalanche photodiodes (APDs).
http://dx.doi.org/10.1364/OL.39.004204

Although Si-based optoelectronic devices have attracted much attention due to their low cost and compatibility with a complementary metal oxide semiconductor, there is still a strong drive to utilize Ge for integrating a photodetector (PD) in optical communication circuits. This is because Ge has an excellent absorption property in the frequency band ($\lambda = 1.3$ μm or 1.55 μm) for optical communication. Recently, the concept of an avalanche photodetector (APD) to achieve high internal gain and, consequently, to detect low-power optical signals has been researched on Ge on Si substrate. Most of works have exploited Ge only for the light absorption layer and Si for the carrier multiplication region, consequently demonstrating maximum multiplication gains (M) of 30–400 at the voltage range of 26–30 V [1–3]. These APDs also presented that the impact ionization phenomenon was initiated at around 18 V due to the wider energy bandgap (1.12 eV) of Si than Ge (0.66 eV).

In the case of Ge APDs, which use only Ge for light absorption and carrier multiplication regions, low gain ($M = 10$) was reported at a low operating voltage of 1.5 V, based on the metal-semiconductor-metal (MSM) type device structure [4]. However, Ge MSM PDs generally suffer from the high dark current caused by a lower hole barrier height because metal-induced gap states lead to Fermi-level pinning close to the Ge valence band [5]. Even though an n-type Ge can be used to take advantage of the Fermi level pinning effect, low electron barrier height (~0.56 eV), due to its low-energy bandgap, still results in a dramatic increase in dark current for the APD under the impact ionization mechanism. Unfortunately, p-i-n Ge PDs are also not free from the high dark current problem caused by point defects, which are created during an ion implantation process. Generation current through these point traps, which did not completely heal during activation process, subsequently acts to increase the dark current [6]. In order to achieve Ge APDs with high M value and high detectivity (D^*) at a low operating voltage, it is necessary to minimize the dark current as well as the avalanche breakdown voltage (V_{ABR}) where the impact ionization process is triggered. In this Letter, we demonstrate a Ge p-i-n APD with a low dark current, low operating voltage (also, a low V_{ABR}), and high gain by (1) minimizing the point defects within the Ge crystal and (2) adjusting the doping concentration of the intrinsic region.

Figure 1 presents the schematic diagram of the Ge p-i-n APD structure and its energy-band diagram under operation. About 1 μm thick intrinsic Ge film was heteroepitaxially grown on Si substrate, followed by a 15 nm thick SiO_2 deposition step at room temperature in an atomic layer deposition (ALD) system. We then defined the p- and n-well regions by performing boron (B) and phosphorus (P) implantation processes. B ions were

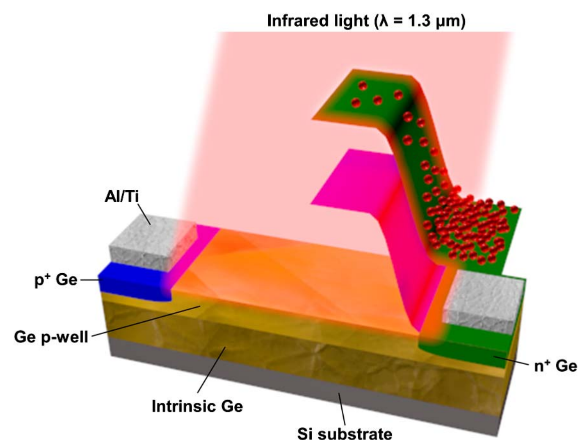

Fig. 1. Schematic diagram presenting Ge p-i-n APD structure and its energy-band diagram under operation.

0146-9592/14/144204-04$15.00/0 © 2014 Optical Society of America

implanted at 60 keV with different doses of 3×10^{11} cm^{-2} to 3×10^{13} cm^{-2}, corresponding to 10^{16} cm^{-3} to 10^{18} cm^{-3}. For comparison purpose with the p-well sample doped at 10^{17} cm^{-3}, an n-well was made with P ion implantation at 160 keV energy and 2×10^{12} cm^{-2} dose. The depth of the p- and n-well (X_{jw}) is about 300 nm. After the well implantation steps, n^+ and p^+ regions were separately patterned by photolithography. Then arsenic (As) and B ions were implanted separately with a dose of 10^{15} cm^{-2} at 60 and 20 keV, respectively, to form the n^+ and p^+ regions with 60 nm of junction depth (X_{jc}). The length (L) between p^+ and n^+ regions is 20 μm, and the width (W) of the p^+ and n^+ regions is 70 μm. In order to activate the implanted dopants and heal the generated point defects, the samples were annealed from 550°C to 650°C in an N_2 ambient for 1 h. Then the damaged SiO_2 layer was removed by a diluted buffered oxide etchant. 20 nm thick Ti and 200 nm thick Al films were subsequently deposited over the whole area on the samples patterned by the photolithography process, and the films outside the metal contact regions were removed by a lift-off process. Finally, dark and photo I-V characteristics of the Ge p-i-n APDs were measured with an infrared laser source ($\lambda = 1.3$ μm and $P = 0.25$ mW). In addition, Raman spectroscopy and electrochemical capacitance voltage (ECV) analyses were performed to investigate the junction interfaces in more detail.

Figures 2(a) and 2(b) show the dark I-V characteristics of Ge $n^+/p/p^+$ and $p^+/n/n^+$ junctions with a body (or well) concentration of 10^{17} cm^{-3}, which were annealed from 550°C to 650°C. Since the point defects that cause the generation current were not healed at 550°C, very high dark current, depending on a junction bias, was observed [Fig. 2(a)]. However, the dark current was dramatically reduced after performing above 600°C anneal. As we confirmed in the previous report [6], most of point defects generated during the implantation process seem to successfully heal after a high-temperature anneal. In the case of the 600°C annealed $n^+/p/p^+$ junction, a slightly lower dark current was observed at the bias region below 1.5 V than in the 650°C sample. It also was increased as a function of a junction bias, indicating that there still exists some point defects inducing a generation current. Although the number of point defects

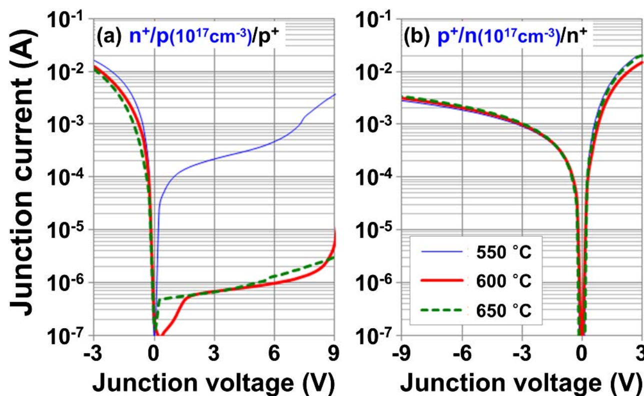

Fig. 2. Dark I-V characteristics of (a) $n^+/p/p^+$ and (b) $p^+/n/n^+$ junctions, which were annealed at 550°C, 600°C, and 650°C.

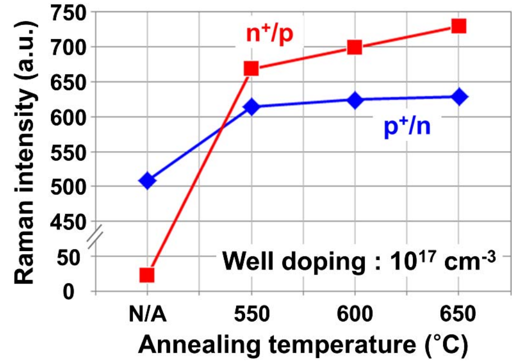

Fig. 3. Raman intensity of Ge peaks extracted in the n^+/p and p^+/n samples, which were nonannealed and annealed at 550°C, 600°C, and 650°C.

was more reduced after the 650°C anneal, deeper diffusion of As atoms from the n^+ region to the body seems to increase the diffusion current due to the nonuniform body doping profile near the junction interface. Meanwhile, in the annealed $p^+/n/n^+$ junctions, very high dark currents were observed, not showing the point defect healing phenomenon. We predict that a too-high implantation energy (160 eV) of P ions for the n-well caused more severe crystal damage in Ge, consequently requiring higher thermal energy to heal the defects.

In order to support our previous claims about the point defect healing, Raman analysis was performed on the Ge $n^+/p/p^+$ and $p^+/n/n^+$ junctions with a body (or well) concentration of 10^{17} cm^{-3} (Fig. 3). In the as-implanted samples, a low peak intensity was observed, and, especially, the peak intensity in the $n^+/p/p^+$ sample was relatively much lower. It is because As ions are much heavier than B ions, subsequently causing more severe crystal damage. Besides, compared with the Raman peak position (303 cm^{-1}) measured on a bulk Ge substrate, a redshift of peaks (meaning a tensile stress of Ge crystal structure) was clearly observed in the as-implanted junctions (272.4 cm^{-1} for $n^+/p/p^+$ and 300.2 cm^{-1} for $p^+/n/n^+$). The much bigger shift in the $n^+/p/p^+$ sample is coincident with the lower peak intensity caused by more severe crystal damage. With annealing, the peak intensity increased, and the peak position also returned back to the initial position since the crystal damage was gradually healed as the annealing temperature increased. Due to the high-energy implantation of P ions for the n-well (or body) region, $p^+/n/n^+$ samples presented lower peak intensity and lower peak position than $n^+/p/p^+$ samples after the anneal between 550°C and 650°C. Here the peak positions (302.7 cm^{-1} at 550°C, 302.8 cm^{-1} at 600°C, and 303 cm^{-1} at 650°C) of the annealed $n^+/p/p^+$ samples were very close to that of bulk Ge.

We then extracted the V_{ABR} values and dark currents (at $V_R = 1$ V) in the p-i-n APD devices fabricated on three different p-wells (10^{16} cm^{-3}, 10^{17} cm^{-3}, and 10^{18} cm^{-3}) and annealed at 550°C, 600°C, and 650°C, as seen in Fig. 4. We also note that the V_{ABR} was defined as the voltage where a photocurrent was increased by 110%. As the body doping concentration increased, V_{ABR} was dramatically reduced from 38 to 2.2 V in the 650°C annealed samples because V_{ABR} is inversely

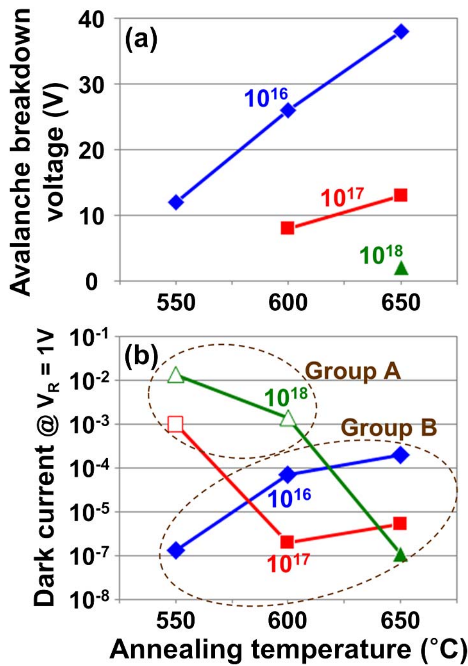

Fig. 4. (a) Avalanche breakdown voltages (V_{ABR}) and (b) dark currents at $V_R = 1$ V of $n^+/p/p^+$ junctions, which were fabricated on three different p-wells (10^{16} cm^{-3}, 10^{17} cm^{-3}, and 10^{18} cm^{-3}) and annealed at 550°C, 600°C, and 650°C.

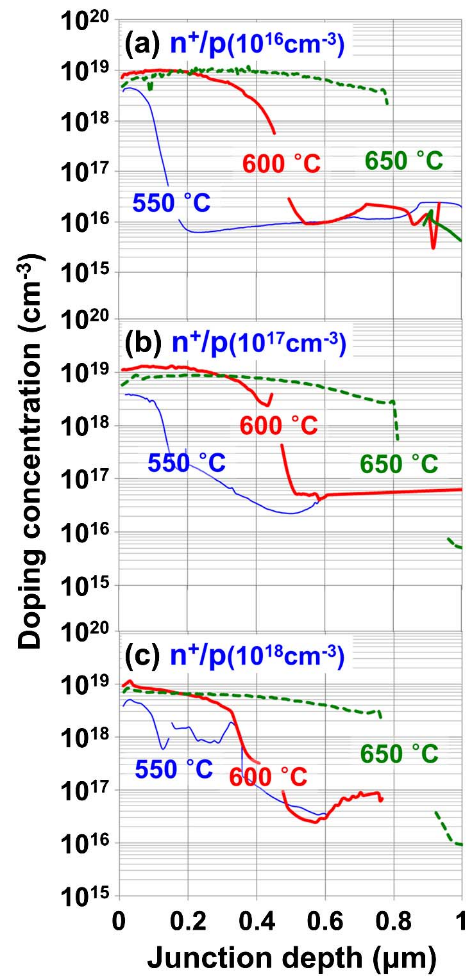

Fig. 5. (ECV analysis) Doping concentrations as a function of junction depth in the n^+/p junctions, which were fabricated on three different p-wells (10^{16} cm^{-3}, 10^{17} cm^{-3}, and 10^{18} cm^{-3}) and also annealed at 550°C, 600°C, and 650°C.

proportional to body doping concentration in asymmetrically doped junctions. In addition, V_{ABR} showed an increasing tendency as the annealing temperature became higher. At higher annealing temperature, the diffusion of As atoms into the deeper p-well region where lower B concentration exists are expected to increase V_{ABR}. As shown in Fig. 4(b), we also compared the dark currents at $V_R = 1$ V, which were extracted from the APD devices. The devices in group A presented very high dark currents because the point defects created by the ion implantation process were not sufficiently healed. Due to this high dark current by tunneling mechanism through the point defects, the avalanche breakdown phenomenon was masked, as shown in Fig. 4(a). Meanwhile, very low dark currents were obtained in group B, where the point defects were successfully annihilated. In the case of group B devices, the diffusion current seems to be more dominant than the generation current because the defects causing the generation current were mostly removed. Since diffusion current is inversely proportional to the body doping concentration, a lower dark current was observed in the junctions fabricated on a higher doped body substrate. Especially, the dark current increased as a function of the annealing temperature in the same body doping concentration. As we have previously mentioned, this also can be explained by deeper diffusion of As and consequently lower B concentration of the body-side near the junction interface.

As seen in the ECV concentration profiles of Fig. 5, As atoms seem to have diffused deeper from the ~0.17 μm to ~0.8 μm region when the anneal temperature was increased from 550°C to 650°C because of their high diffusivity in Ge [7]. In addition, nonuniform profiles of B atoms were confirmed in the body (well) region since the implanted B atoms were dispersed by a Gaussian distribution function, and they were known to possess very low diffusivity in Ge [8]. The highest activation percentage (46.50% of the implanted dose) of As was observed after 600°C anneal, indicating that the annealing above 600°C is required for the successful As dopant activation. But it is confirmed that if the annealing process temperature gets too high (above 650°C), it causes a severe dopant loss through the outdiffusion phenomenon of As atoms. In the other samples, slightly lower activation percentages of 9.92% at 550°C and 32.80% at 650°C were obtained, respectively owing to the insufficient thermal energy for activation and the dopant loss by outdiffusion.

As shown in Fig. 6, the photo/dark I-V characteristics were then measured with an infrared laser ($\lambda = 1.3$ μm and $P = 0.25$ mW) source, and the extracted M values on the p-i-n APD devices were plotted. Here the incident power is predicted to be slightly lower than 0.25 mW because of surface reflection. Figure 6(a) presents the dark and photo I-V characteristics and the extracted M curve of the APD device with a body doping (p-well) concentration of 10^{17} cm^{-3}. We note that the photocurrent is expected to be measured under a mixed injection condition since all of the n^+, p, and p^+ regions in Ge APD can

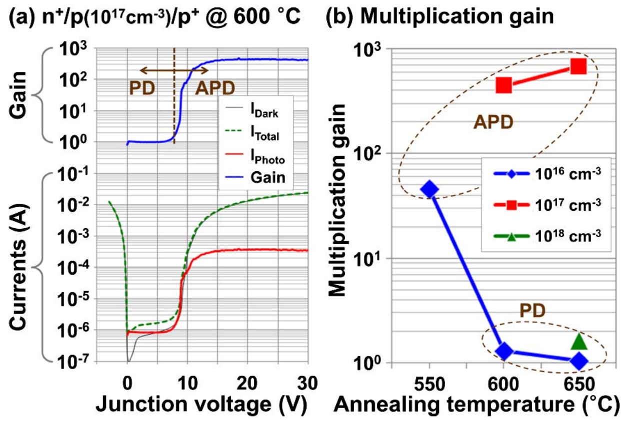

Fig. 6. (a) Photo and dark I-V characteristics including multiplication gain curve of the $n^+/p/p^+$ APD fabricated on 10^{17} cm^{-3} p-type well and annealed at 600°C. (b) Multiplication gain as a function of annealing temperature in the $n^+/p/p^+$ APD devices, which were fabricated on three different p-wells (10^{16} cm^{-3}, 10^{17} cm^{-3}, and 10^{18} cm^{-3}).

absorb the light with a 1.3 μm wavelength, and the light was exposed to the entire surface. As already mentioned in Fig. 4, about 8 V of V_{ABR} was observed, and a dramatically amplified photocurrent reached to ~300 μA at 15 V, showing a high M value of ~400 in the APD operating mode. The calculated M values from Fig. 6(a) were plotted as a function of annealing temperature [Fig. 6(b)]. In the case of low body doping (p-well) devices with 10^{16} cm^{-3}, M values were obtained in all of the junctions because the crystal damages were sufficiently healed through an above 550°C anneal.

However, a wide depletion region and, subsequently, a low maximum electric field in the region made it difficult to achieve high M values. In addition, the diffusion of As atoms to the region with lower B concentration is expected to increase the depletion width, decrease maximum electric field, and finally provide lower M values at the higher-temperature annealed sample. Meanwhile, even though the 550°C annealed sample with body doping of 10^{17} cm^{-3} suffered from a high dark current problem due to insufficient healing, very high M values (~440) were achieved in the other samples annealed above 600° C. The narrowed depletion width by increasing a body doping concentration is predicted to result in a higher maximum electric field and eventually a higher-impact ionization probability. Here, since the maximum electric field intensity in the depletion region is high enough to trigger the impact ionization phenomenon, the additional increase of depletion width by deeper As diffusion at 650° C is expected to increase the M value up to ~680. When the body doping concentration was increased up to 10^{18} cm^{-3}, a very low M value was obtained due to the strong tunneling phenomenon [9]. We also predict that saturation phenomenon in the dark- and photocurrent is attributed to the series resistance effect, which typically induces a current saturation in the forward biased region.

In conclusion, we presented Ge p-i-n APDs with a low dark current (sub 1 μA below $V_R = 5$ V), low operating voltage ($V_{ABR} = 8$–13 V), and high gain (440–680) by exploiting the point defect healing method (between 600°C and 650°C) and optimizing the doping concentration of the intrinsic region (p-type ~10^{17} cm^{-3}). This successful demonstration of Ge p-i-n APDs with low dark current, low V_{ABR}, and high M is promising for low-power and high-sensitivity Ge PD applications.

This research was supported by the Basic Science Research Program and Mid-career Researcher Program through the National Research Foundation of Korea (NRF) funded by the Ministry of Education, Science, and Technology (NRF-2011-0007997 and 2012R1A2A2A02046890).

References

1. M. S. Carrol, K. Childs, R. Jarecki, T. Bauer, and K. Saiz, Appl. Phys. Lett. **93**, 183511 (2008).
2. Y. Kang, H.-D. Liu, M. Morse, M. J. Paniccia, M. Zadka, S. Litski, G. Sarid, A. Pauchard, Y.-H. Kuo, H.-W. Chen, W. S. Zaoui, J. E. Bowers, A. Beling, D. C. Mclntosh, X. Zheng, and J. C. Campbell, Nat. Photonics **3**, 59 (2008).
3. N. Duan, T.-Y. Liow, A. E.-J. Lim, L. Ding, and G. Q. Lo, Opt. Express **20**, 11031 (2012).
4. S. Assefa, F. Xia, and Y. A. Vlasov, Nature **464**, 80 (2010).
5. T. Nishimura, K. Kita, and A. Toriumi, Appl. Phys. Lett. **91**, 123123 (2007).
6. J. Shim, J.-H. Shin, I.-Y. Lee, D. Choi, J. W. Baek, J. Heo, W. Park, J. W. Leem, J. S. Yu, W.-S. Jung, K. Saraswat, and J.-H. Park, Jpn. J. Appl. Phys. **114**, 094515 (2013).
7. S. Koffel, R. J. Kaiser, A. J. Bauer, B. Amon, P. Pichler, J. Lorenz, L. Frey, P. Scheiblin, V. Mazzocchi, J.-P. Barnes, and A. Claverie, Microelectron. Eng. **88**, 458 (2011).
8. Y. S. Suh, M. S. Carroll, R. A. Levy, A. Sahiner, and C. A. King, Mater. Res. Soc. Symp. Proc. **809**, B8.11.1 (2004).
9. R. F. Pierret, *Semiconductor Device Fundamentals* (Addison-Wesley, 1996).